Supporting Information

A Facile Strategy for Preparing Porous Cu_2O Nanosphere and Application as Nanozymes in Colorimetric Biosensing

Ying Zhu Zhilu Zhang Xinyu Song* Yuxiang Bu

School of Chemistry and Chemical Engineering, Shandong University, Jinan, 250100, Peoples' Republic of China

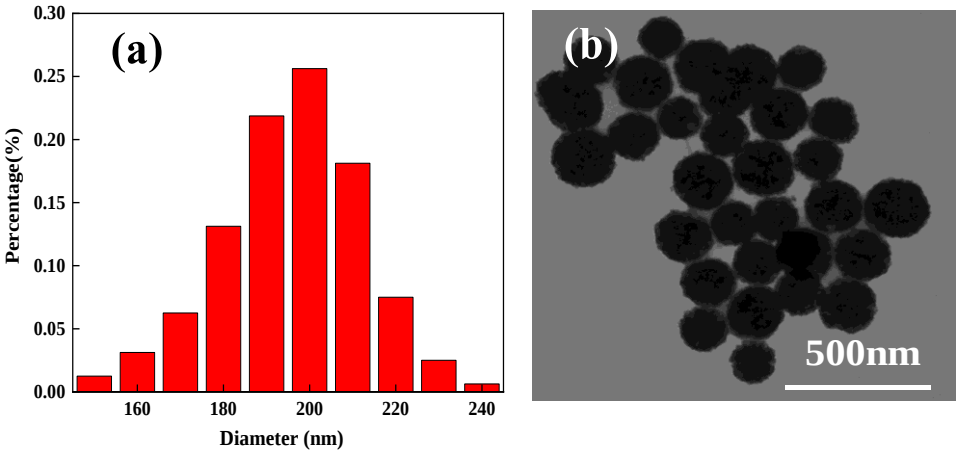

Fig. S1. (a) size distribution of Cu_2O NPs. (b) TEM image of Cu_2O NPs.

* E-mail: songxy@sdu.edu.cn

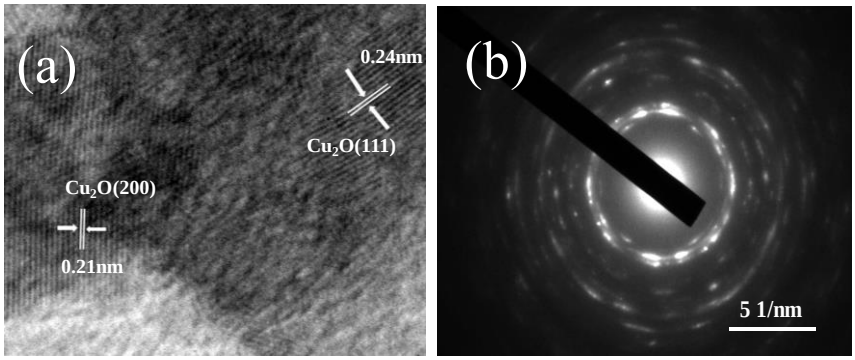

Fig. S2. (a) HR-TEM image of the Cu_2O NPs showing the interplanar spacing. (b) SAED patternd of Cu_2O NPs.

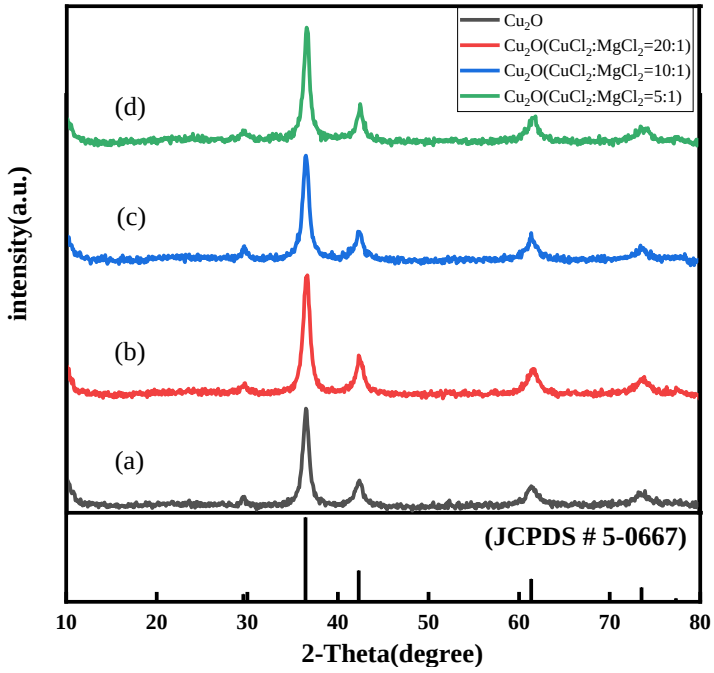

Fig. S3. XRD of Cu_2O NPs of different molar ratio of $CuCl_2$:$MgCl_2$: (a) sole $CuCl_2$. (b) 20:1, (c) 10:1, (d) 5:1.

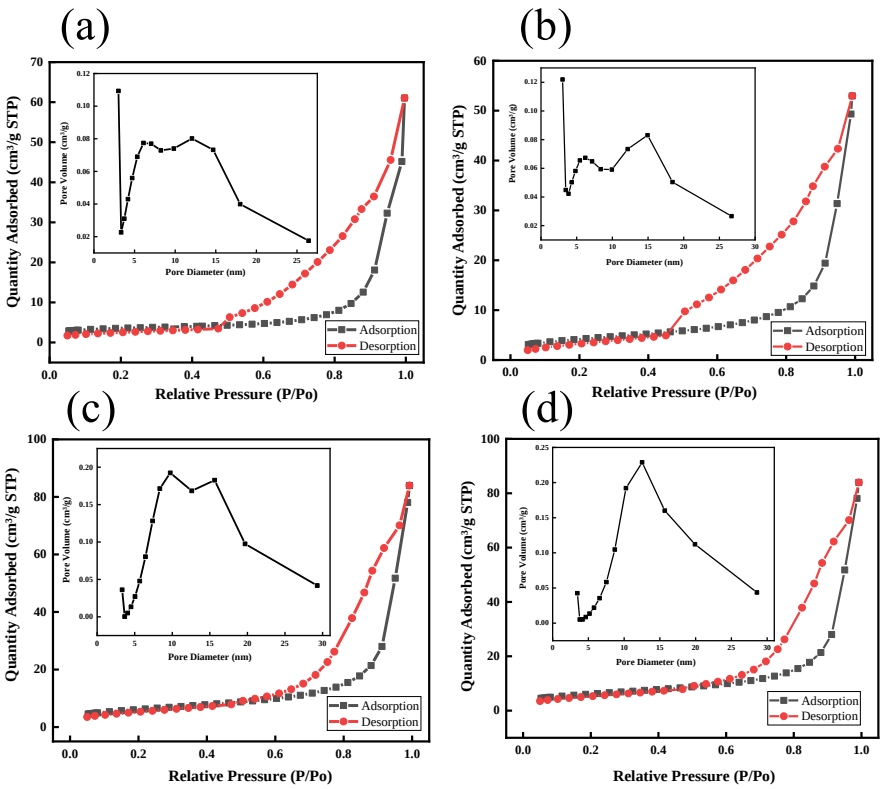

Fig. S4. BET analysis of Cu_2O of prepared with different molar ratio of $CuCl_2$:$MgCl_2$ (inset: pore size distribution (BJH-method)): (a) sole $CuCl_2$, (b) 20:1, (c) 10:1, (d) 5:1

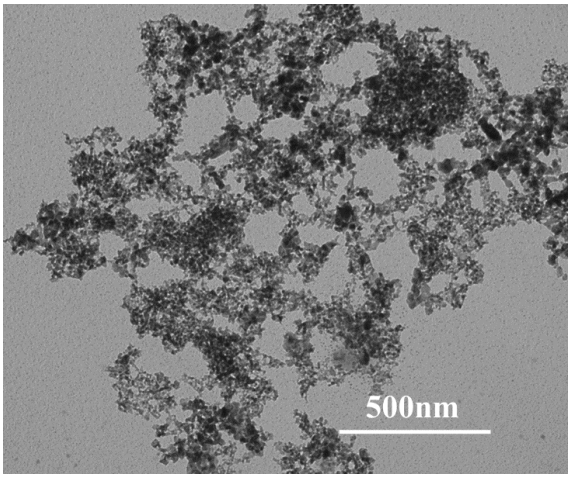

Fig. S5. TEM image of the Cu-precursors without adding $MgCl_2$

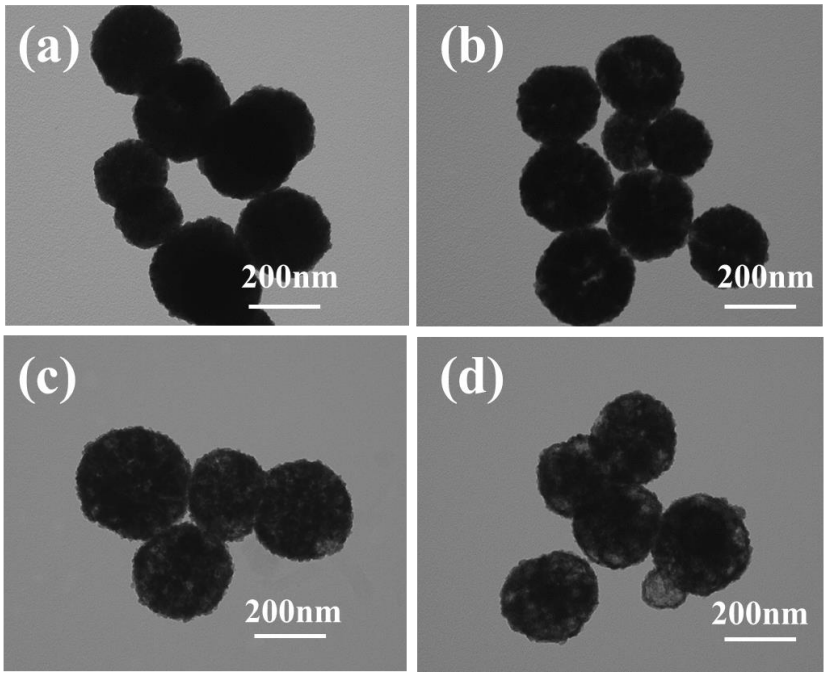

Fig. S6. TEM images of the formation process of Cu_2O-(10:1-Mg): (a) 5 min, (b) 10 min, (c) 20 min, (d) 40 min.

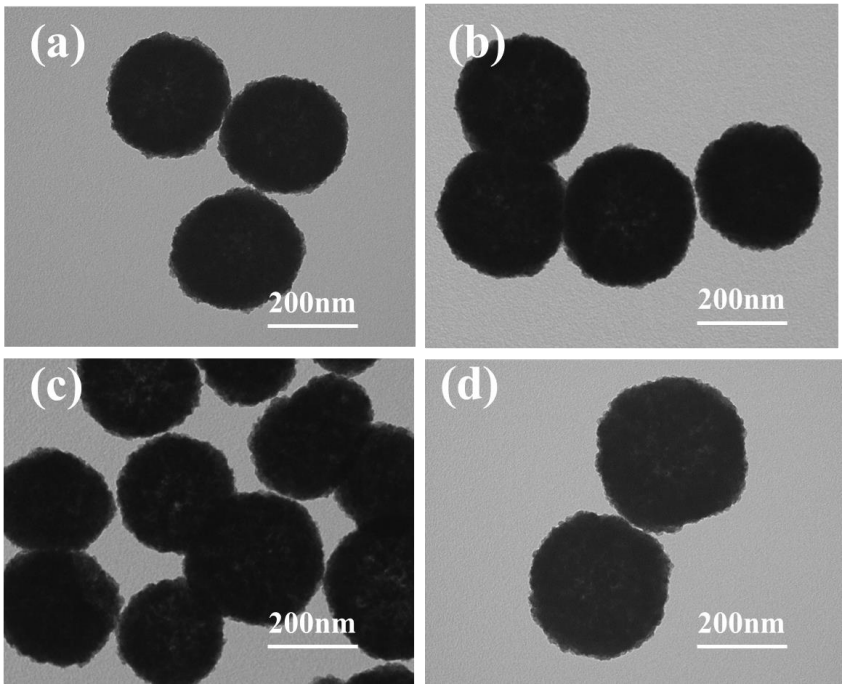

Fig. S7. TEM images of the formation process of Cu_2O-(sole $CuCl_2$): (a) 5 min, (b) 10 min, (c) 20 min, (d) 40 min.

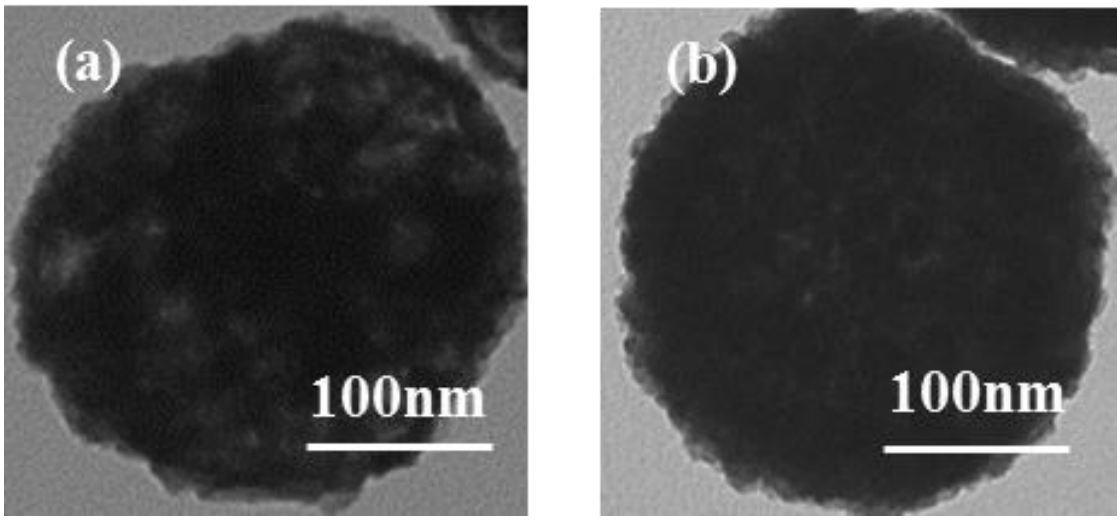

Fig. S8. The magnified TEM image (a) Cu_2O-(10:1-Mg) NPs,
(b) Cu_2O-(sole $CuCl_2$) NPs

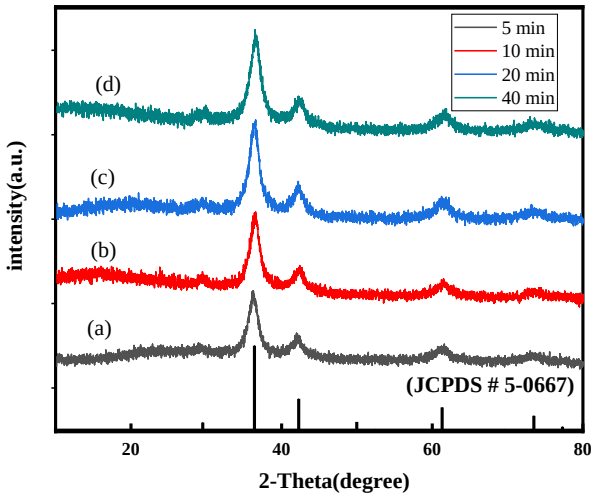

Fig. S9. XRD of the formation process of Cu_2O-(10:1-Mg): (a) 5 min, (b) 10 min,
(c) 20 min, (d) 40 min.

In the sample preparation for ICP analysis, the cuprous oxide was accurately weighed, dissolved in 1ml deionized water and diluted 10000 times. Finally, the analysis solution obtained before adding 2% up-HNO_3.

Table S1. Mass content of Mg in the Cu_2O-(10:1-Mg) determined by ICP-MS

Sample	Mg Concentration(ppm)	Wt%
5 min	11.143	1.1%
40 min	0.046	0.005%

Table S2. pH value during the reduction reaction process

Time	pH
0	7.43
5	6.97
10	6.44
20	6.20
30	6.16
40	6.13
60	6.13

Table S3. Zeta potential of the various Cu_2O samples

Samples	Zeta potential
Cu_2O-(sole $CuCl_2$)	-12.4 mV
Cu_2O-(20:1-Mg)	-14.5 mV
Cu_2O-(10:1-Mg)	-17.6 mV
Cu_2O-(5:1-Mg)	-18.1 mV

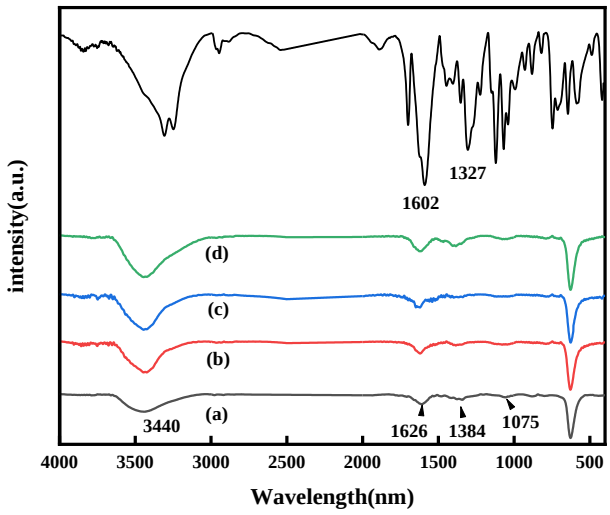

Fig. S10. FT-IR spectroscopy of the synthesized NPs of different molar ratio of $CuCl_2$:$MgCl_2$: (a) sole $CuCl_2$, (b) 20:1, (c) 10:1, (d) 5:1.

Table S4. Comparison of the Michaelis–Menten Constant and Maximal Velocity of different nanomaterials.

Catalyst	Substrate	K_m (mM)	V_m (M S^{-1})	*Ref.*
HRP	TMB	0.434	10.0×10^{-8}	[1]
	H_2O_2	3.70	8.71×10^{-8}	
DNA/CuAl-LDH	TMB	1.775	4.09×10^{-8}	[2]
	H_2O_2	10.24	2.3×10^{-8}	
$CePO_4$–CeO_2	TMB	0.23	8.78×10^{-8}	[3]
	H_2O_2	4.76	29.79×10^{-8}	
Brominated Graphene	TMB	0.83	0.68×10^{-8}	[4]
	H_2O_2	10.98	3.60×10^{-8}	
VO_2(A) nanoplates	TMB	0.165	2.4×10^{-8}	[5]
	H_2O_2	0.058	1.4×10^{-8}	
TiO_2@CeO_x	TMB	0.28	0.65×10^{-8}	[6]
	H_2O_2	6.29	3.4×10^{-8}	
Cu_2O-(sole $CuCl_2$)	TMB	0.256	7.58×10^{-9}	This work
	H_2O_2	0.860	1.81×10^{-8}	
Cu_2O-(10:1-Mg)	TMB	0.128	1.11×10^{-8}	This work
	H_2O_2	0.729	2.68×10^{-8}	

■ References

[1] S. Jain, B. Sharma, N. Thakur, S. Mishra and T. K. Sarma, *ACS Appl. Nano Mater*., 2020, **3**, 8, 7917–7929.

[2] L. Chen, K. Sun, P. Li, X. Fan, J. Sun and S. Ai, *Nanoscale*, 2013, **5**, 10982-10988.

[3] G. Vinothkumar, A. I. Lalitha and K. Suresh Babu, *Inorg. Chem*., 2019, **58**, 349-358.

[4] S. Singh, K. Mitra, R. Singh, A. Kumari, S. K. Sen Gupta, N. Misra, P. Maiti and B. Ray, *Anal. Methods*, 2017, **9**, 6675-6681.

[5] L. Zhang, F. Xia, Z. Song, N. Webster, H. Luo and Y. Gao, *RSC Adv*., 2015, **5**, 61371-61379.

[6] L. Artiglia, S. Agnoli, M. Paganini, M. Cattelan and G. Granozzi, *ACS Appl. Mater. Inter*., 2014, **6**, 20130-20136.

[7] C. Chen, Y. Wang and D. Zhang, *Microchim. Acta*, 2019, **186**, 784.

[8] M. Singh, P. Weerathunge, P. D. Liyanage, E. Mayes, R. Ramanathan and V. Bansal, *Langmuir*, 2017, **33**, 10006-10015.

[9] Y. Chen, T. Chen, X. Wu and G. Yang, *Sensor Actuat. B: Chem*., 2019, **279**, 374-384.

[10] C. Jiang, X. Wei, S. Bao, H. Tu and W. Wang, *RSC Adv*., 2019, **9**, 41561-41568.

ESR spectrum. Specifically, 100 μL of Cu_2O NPs with different concentrations, 100 μL of 20 mM DMPO and 100 μL of 5 mM H_2O_2 were added into a plastic tube, and then the prepared sample solution was transferred to a quartz capillary tube and placed in the ESR cavity. The mixture was quickly measured by recording the ESR spectrum.

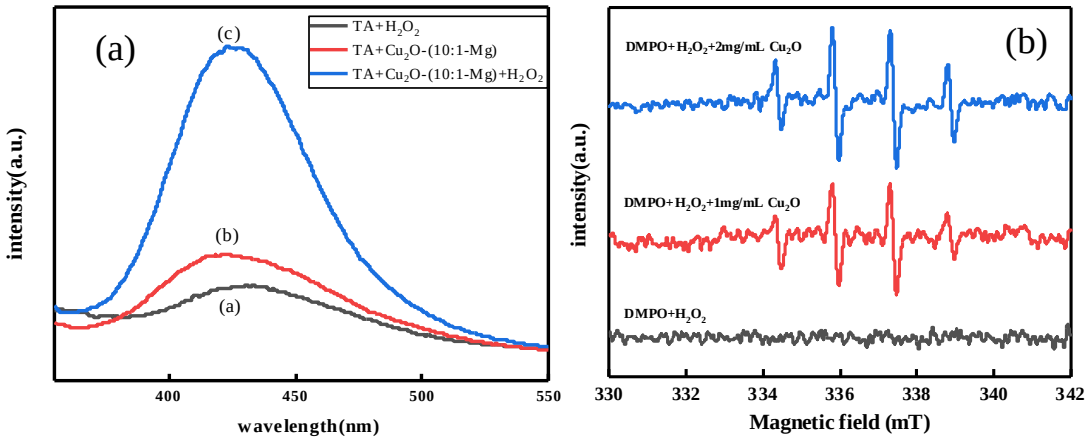

Fig. S11. (a) Fluorescence spectrum of (a) TA + H_2O_2, (b) TA + Cu_2O-(10:1-Mg), (c) TA + Cu_2O-(10:1-Mg) + H_2O_2. (b) ESR spectra of the DMPO/·OH spin adduct at different concentrations of Cu_2O NPs.

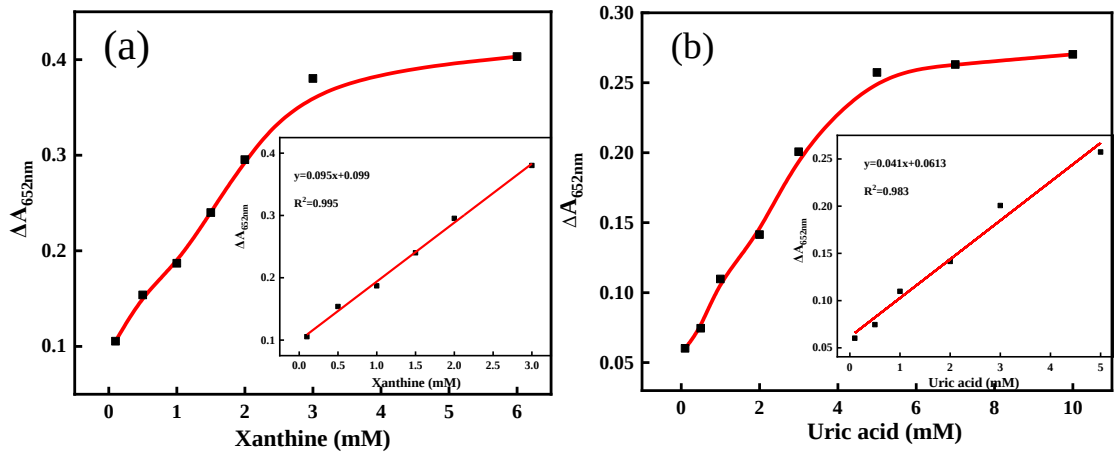

Fig. S12. The dependency of the absorbance at 652 nm on the concentrations of xanthine (a) and uric acid (b).

Table S5. Detection of the glucose standard added to human serum samples

Samples	Found value (mM)	Added (mM)	Found value (mM)	Recovery (%)	RSD (%)	Hospital method(mM)
1	5.74	0.2	5.82	98.0	1.2	5.67
2	5.59	0.4	6.08	101.5	2.0	5.52
3	5.88	1.0	6.80	98.9	0.9	5.90

Real sample analysis. For real sample analysis, glucose content in human serum samples was detected with the same methodology. The serum samples from healthy adults collected from the local hospital were first centrifuged at 12000 rpm, and then the supernatants were diluted by 10 folds. The detection procedure was the same as that of glucose in the buffer solution mentioned above, and the results were compared with those obtained by BS-380 automatic biochemical analyzer used in hospitals.

Table S6. Comparison of various nanomaterials employed for the detection of L-cysteine.

Material	LOD (μM)	Linear range (μM)	Refs.
VS_4	0.97	0-100	[7]
$Gd(OH)_3$ nanorods	2.6	0.2–75	[8]
$CuMnO_2$ nanoflakes	11.26	25–300	[9]
R-Cu@Au/Pt NPs	4.0	0–400	[10]
Cu_2O-(10:1-Mg)	0.81	0-10	This work

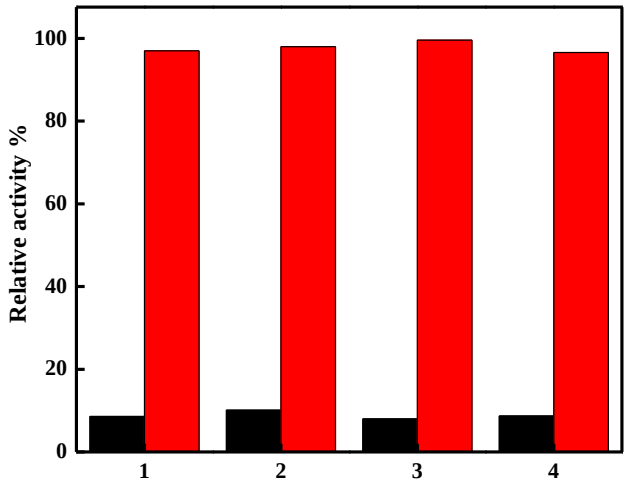

Fig. S13. Selectivity analysis for L-cysteine detection in the presence of other thiol-containing molecules, the black bars and red bars represent the system in the presence and absence of L-cysteine, respectively. (1) Met, (2) cystine, (3) cystamine, (4) homocysteine.

Table S7 Analysis of real samples with different concentrations of L-cysteine

Samples	Added (μM)	Found (μM)	Recovery (%)	RSD (%)
1	4	4.12	103	2.3
2	6	5.87	97.8	1.4
3	8	7.79	97.4	1.6

The serum samples filtrates were spiked with standard L-cysteine solutions at certain concentrations, and added into the mixture composed by the Cu_2O NPs+TMB+H_2O_2. After that, L-cysteine was detected using a UV-vis spectrophotometer as mentioned above.